Supermodeling: Synchronization of Alternative Dynamical Models of a Single Objective Process

Gregory S. Duane[1,2], Wim Wiegerinck[3], Frank Selten[4], Mao-Lin Shen[1], and Noel Keenlyside[1]

Abstract Imperfect models of the same objective process give an improved representation of that process, from which they assimilate data, if they are also coupled to one another. Inter-model coupling, through nudging, or more strongly through averaging of dynamical tendencies, typically gives synchronization or partial synchronization of models and hence formation of consensus. Previous studies of supermodels of interest for weather and climate prediction are here reviewed. The scheme has been applied to a hierarchy of models, ranging from simple systems of ordinary differential equations, to models based on the quasi-geostrophic approximation to geophysical fluid dynamics, to primitive-equation fluid dynamical models, and finally to state-of-the-art climate models. Evidence is reviewed to test the claim that, in nonlinear systems, the synchronized-model scheme surpasses the usual procedure of averaging model outputs.

I. Introduction

It has been established that a computational model that runs in parallel to the objective process being modeled can be conceived as synchronizing with that process through a one-way truth-model coupling [9,31]. In numerical weather prediction, the repeated updates of the model based on new observations constitute the enterprise of *data assimilation*, methods for which are well developed in meteorology [13]. It can indeed be shown that Kalman Filtering, the algorithm that provides the basis for the most common data assimilation methods, is also optimal for synchronization of truth and model under weak assumptions of local linearity [9].

Similarly, a biological organism perceives reality through a stream of incoming data and forms a prognostically useful perception than synchronizes with, but is distinct from objective reality. A conscious organism exhibits an additional feature: it perceives itself, focusing on its own thoughts in the same manner as it does

[1] Geophysical Institute, University of Bergen, Norway
[2] Department of Atmospheric and Oceanic Sciences, University of Colorado, Boulder, USA
[3] Department of Medical Physics and Biophysics, Radboud University, Nijmegen, The Netherlands
[4] Royal Netherlands Meteorological Institute (KNMI), De Bilt, The Netherlands

the objective world. In this view, there must be semi-autonomous parts of a "conscious" mind that perceive one another. These components of the mind synchronize with one another, or in alternative language, they perform "data assimilation" from one another, with a limited exchange of information, lending an additional degree of objectivity to a conscious organism.

Such a scheme has actually been proposed in a computational science context, for the fusion of alternative computational models of the same objective process [8, 27,19]: different numerical models used to predict climate change in the 21st century differ by as much as a factor of two in the amount of globally-averaged warming and differ completely in their projections for specific regions of the globe. Current practice is just to average the results of the different models. By synchronizing a small set of alternative models with each other, a more reliable and detailed consensus could be obtained.

The supermodel strategy is schematized in Figure 1, for three constituent models. The three models perform data assimilation from (synchronization with) reality, through diffusive coupling with coefficient matrices K^i ("Kalman gains" in the language of data assimilation).

The l^{th} variable in Model i is nudged to the l^{th} variable in Model j with connection coefficient C_l^{ij}.The connections C_{ij} linking the three model systems can be chosen using yet a further extension of the synchronization paradigm: if two systems synchronize when their parameters match, then under some weak assumptions, as was proven in [9], it is possible to prescribe a dynamical evolution law for general parameters in one of the systems, so that the parameters of the two systems, as well as the states will converge. In the present case, the tunable parameters are taken to be the connection coefficients (not the parameters of the separate models), and they are tuned under the peculiar assumption that reality itself is a similar suite of connected systems.

In the following sections, we present the results of the supermodeling approach in a hierarchy of increasingly complex models. Details of the learning algorithm are reviewed in the next section, for simple examples where the models are sets of a few ordinary differential equations. In Section 3, the strategy is applied to a partial differential equation model, the quasigeostrophic channel model, where the advantages of supermodeling can be clearly compared to *ex post facto* averaging. In section 4 it is shown that the scheme can be applied to a fluid dynamical model capturing realistic features of the climate system. Preliminary efforts with state-of –the-art climate models are reviewed in Section 5, and the overall status of supermodelling is summarized in Section 6.

II. Supermodeling with Low-Order Models

A simple supermodel is constructed from a collection of Lorenz systems [17] that each imperfectly represent a "true" Lorenz system. Three imperfect "model" Lorenz systems were generated by perturbing parameters in the differential equations for a given "real" Lorenz system and adding extra terms. The resulting suite is: $dx/dt = \sigma(y-z)$, $dy/dt = \rho x - y - xz$, $dz/dt = -\beta z + xy$, and

$$\begin{aligned} dx_i/dt &= \sigma_i(y_i - z_i) + \sum_{j\neq i} C^x_{ij}(x_j - x_i) + K^x(x - x_i) \\ dy_i/dt &= \varrho x_i - y_i - x_i z_i + \mu_i + \sum_{j\neq i} C^y_{ij}(y_j - y_i) + K^y(y - y_i) \\ dz_i/dt &= -\beta_i z_i + x_i y_i + \sum_{j\neq i} C^z_{ij}(z_j - z_i) + K^z(z - z_i) \end{aligned} \qquad (1)$$

where (x, y, z) is the real Lorenz system and (x_i, y_i, z_i) $i = 1, 2, 3$ are the three models. An extra term μ is present in the models, but not in the real system. Because of the relatively small number of variables available in this toy system, all possible directional couplings among corresponding variables in the three Lorenz systems were considered, giving 18 connection coefficients C^A_{ij} $A = x, y, z$; $i, j = 1, 2, 3$, $i \neq j$. The constants K^A $A = x, y, z$ are chosen arbitrarily so as to effect "data assimilation" from the "real" Lorenz system into the three coupled "model" systems.

It remains to determine connection coefficients C^A_{ij} that will define an optimal supermodel. The general method for parameter adaptation in any imperfect replica of any dynamical system with which the imperfect replica synchronizes [10], to be applied here, is the following: Consider a "real system" given by ODE's: $dx/dt = f(x, p)$, $dp/dt = 0$, where $x \in R^N$, $f : R^N \to R^N$, and $p \in R^m$ is the vector of (unknown, constant) parameters of the system. Further assume that $s=h(x)$, where $h : R^N \to R^n$, $n \leq N$, is an n dimensional vector representing the experimental measurement output of the system. A "computational model" of the system is given by $dy/dt = f(y,q) + u(y,s)$, $dq/dt = N(y, x - y)$ where $N(y, 0) = 0$, and u is the control signal. Generally, the real system and its model are chaotic; for $u = 0$ the simulation quickly diverges from the real system behavior. The problem is to find a parameter estimation law N, so that $q \to p$, if we are given a control law u such that $y \to x$. Let $e \equiv y - x$ and $r \equiv q - p$. Consider a Lyapunov function $L_o(e)|_{q=p}$ that is positive definite and monotonically decreasing after some time, e.g. $L_o(e) = e^2$. The recipe for the desired N, as proved in [10], is

$$N_j = -\delta_j \Sigma_i [(\partial L_0/\partial e_i)(\partial h_i/\partial r_j)] \qquad (2)$$

where the δ_j are arbitrary positive constants, and $h \equiv f(y,r + p) - f(y - e,p)$. Typically, the first factor in brackets is simply e_i and the second factor is the cofactor of parameter p_j in the dynamical equation for x_i.

Letting the parameters to be estimated be the connection coefficients themselves (not the parameters of the separate models), the dynamical equation for these coefficients was chosen as:

$$dC^X_{ij}/dt = a\,(x_j - x_i)\,(x - \tfrac{1}{3}\Sigma_k x_k) - \varepsilon/(C^X_{ij} - C_{max})^2 + \varepsilon/(C^X_{ij} + \delta)^2 \qquad (3)$$

with analogous equations for C^Y and C^Z, where the adaptation rate a is an arbitrary constant and the extra terms with coefficient ε dynamically constrain all couplings C^A to remain in the range $(-\delta, C_{max})$ for some small number δ. The rule (3) has a simple interpretation: time integrals of the first terms on the right-hand side of each equation give the covariance between truth-model synchronization error, $x - \frac{1}{3}\Sigma_k x_k$, and inter-model "nudging", $x_j - x_i$. We indeed want to increase or decrease the inter-model nudging, for a given pair of corresponding variables, depending on the sign and magnitude of this covariance. The procedure will produce a set of values for the connection coefficients that is at least locally optimal in the multidimensional space of connection values.

Figure 2a shows the results for a simple case in which each of the three model systems contains the "correct" equation for only one of the three variables and "incorrect" equations for the other two [8, 3]. The couplings did not converge, but the coupled suite of "models" rapidly synchronized with the "real" system, even with the adaptation process turned off half-way through the simulation, so that the coupling coefficients $C^A_{i,j}$ subsequently held fixed values. (The three models also synchronized among themselves nearly identically.) The inter-model connections are needed, despite efforts, common in the modeling community [25], to combine only the outputs of independently run models using Bayesian reasoning. The difference between corresponding variables in the "real" and coupled "model" systems was significantly less than the difference using the average outputs of the same suite of models, not coupled among themselves (Figure 2b). Further, without the model-model coupling, the output of the single model with the best equation for the given variable (in this case, z, modeled best by z_1 in Model 1) differed even more from "reality" than the average output of the three models (Figure 2c). Therefore, it is unlikely that any *ex post facto* weighting scheme applied to the three outputs would give results equaling those of the synchronized suite. Internal synchronization within the multi-model "mind" is essential. The choice of semi-autonomous models to be combined is not essential - in a case where no model had the "correct" equation for any variable, results deteriorated only slightly (Figure 2d).

The synchronization-based method for adapting the inter-model connections is only guaranteed to find a supermodel that is *locally* optimal in the space of connection coefficients. It is not yet known whether local optima are an impediment when such a space is high dimensional. However, Mirchev et al. [19] obtained some improvement in another supermodel constructed from Lorenz systems by introducing stochasticity in the training procedure, a commonly used way to escape local optima.

Synchronization-based adaptation of coefficients is a form of machine learning on-the-fly, in which the coefficients typically oscillate wildly. A more stable procedure is to match entire segments of the supermodel trajectory to the real trajectory. One can introduce a cost function for mismatch, such as the one used by van den Berge et al [27]:

$$F(C) = \frac{1}{K\Delta} \sum_{i=1}^{K} \int_{t_i}^{t_i+\Delta} |x_S(C, t) - x_O(t)|^2 \gamma^t \, dt \qquad (4)$$

for a vector C of connection coefficients, defined as normalized sum over K short integrations of length Δ, with initial times t_i, of the squared error between the true trajectory x_0 and the supermodel trajectory x_S. The integration segments were chosen to overlap, so that $\Delta > t_{i+1} - t_i$. The factor γ^t with $0 < \gamma \leq 1$ is introduced to give stronger weight to the errors close to the initial conditions and discount the chaotic internal error growth that is not a result of model imperfections.

Results of trajectory-matching by minimizing (4) for a supermodel formed from imperfect replicas of a "true" Lorenz system are shown in Figure 3. The algorithm is seen to be particularly useful for reproducing the true attractor, even where the attractors of the imperfect models are very different from truth.

III. Supermodeling vs. Output-Averaging in Quasigeostrophic Models

A. Weighted Supermodeling

To investigate supermodeling with more complex models it is useful to consider a generalization arising from a limiting case of the connected supermodeling scheme described above. A class of supermodels in defined by defining the tendency for a given variable as a weighted average of the tendencies for that variable in the different models. That is, the parameters of the supermodel are weights w^l_i, with $w^l_i \geq 0$ and $\sum_i w^l_i = 1$, and the dynamics for the lth variable are given by:

$$dx^l/dt = \sum_i w^l_i f^l_i(\mathbf{x}) \qquad (5)$$

Weighted supermodels can be considered as connected supermodels with infinitely strong connections, i.e. connections of the form κC^i_{ij} with $C^i_{ij}>0$ and $\kappa\to\infty$. Thus the ratios of the large connections remain constant in the limit. In the limit it can be shown that all model states are completely synchronized $x^i_i = x^j_j$, and that the synchronized state follows the weighted averaged dynamics (5) [30].

B. Weighted Supermodels from Quasigeostrophic Models

The question of whether supermodels can exceed the performance of model output averages can now be addressed with models of more realistic complexity. If nonlinearities are strong enough so as to cause bifurcations in the climate systems as GHGs increase, it can be argued that output averaging will be insufficient to capture the effects and that supermodeling would be beneficial. However, there is little evidence for bifurcations of this type in model studies. But even without bifurcations, simple nonlinearity can still make the supermodel superior to an average of model outputs. This is perhaps most easily seen in the case where diagnostic properties depend non-monotonically on system parameters. Suppose we have two models of the form:

$$\begin{aligned} d\mathbf{x}/dt &= F(\mathbf{x}, p_1) \\ d\mathbf{x}/dt &= F(\mathbf{x}, p_2) \end{aligned} \qquad (6)$$

where F is linear in the parameter p, and consider some diagnostic P(p), e.g. mean temperature. Further suppose that $P(p_1) = P(p_2)$, but that for some intermediate value p_i, $p_1 < p_i < p_2$, $P(p_i) > P(p_1) = P(p_2)$. Then any weighted average of model outputs will only give the first value $P(p_1)$. A weighted supermodel, on the other hand, could readily reproduce the correct dynamics, that is $F(\mathbf{x}, p_i) = w_1 F(\mathbf{x}, p_1) + w_2 F(\mathbf{x}, p_2)$ for appropriately chosen weights w_1 and w_2, since F is linear in p. It is hypothesized that a connected supermodel could also give the correct result.

Consider specifically a quasigeostrophic model of a re-entrant channel on a β-plane given by:

$$Dq_i/Dt \equiv \partial q_i/\partial t + J(\psi_i, q_i) = F_i + D_i \qquad (7)$$

where the layer i=1,2, ψ is streamfunction, and the Jacobian $J(\psi_i, q_i)$ gives the advective contribution to the Lagrangian derivative D/Dt [29,28]. The forcing F is a relaxation term designed to induce a jet-like flow near the beginning of the channel:

$$F_i = \mu_0 (q_i^* - q_i) \qquad (8)$$

for q_i^* corresponding to a streamfunction ψ^* that defines a jet . The dissipation terms D, boundary conditions, and other parameter values are given in [7].

The QG channel model vacillates between two dynamical regimes corresponding to "blocked" and "zonal" flow, as illustrated in Fig. 4. The response of the blocking activity to the forcing parameter μ_0 in (8) provides a simple example of non-monotonic behavior. For zero forcing, blocking frequency is zero due to damping by the dissipative terms. For large forcing, the flow is consistently jet-like, and again there is no blocking. Typical flow fields for these two cases are shown in Fig. 5a,b. (The zero-forcing flow in Fig. 5a is turbulent, but of low amplitude, and includes no blocks.)

A weighted supermodel formed from the two individual models illustrated in Fig. 5 can reproduce the true dynamics exactly for any value of the forcing coefficient μ_0 between $\mu_0 = 0$ and $\mu_0 = 3$, because μ_0 appears linearly in the tendency and so averaging tendencies effectively averages the μ_0 values [4]. For the typical value $\mu_0 = 0.3$ used previously, the behavior is as illustrated in Fig. 6. The supermodel flow spends much time in the blocked regime, unlike the flows in the individual models or any weighted average thereof. (If the actual flow fields of the individual models are averaged, instead of the blocking frequencies, the same conclusion is reached.)

The learning task for the weights is equivalent to that for determining the single parameter μ_0 directly. The algorithm described in the previous section for parameter learning in models that synchronize with identical parameters [10], for instance, is effective in the present context. While the argument applies exactly to a weighted supermodel, it seems likely that a connected supermodel could also be formed from the two individual models illustrated in Fig. 5 that would approximate the "true" behavior for arbitrary forcing coefficient.

While a supermodel is clearly superior to an output average in the example given above, and in extreme cases generally, more linear behavior is expected for smaller inter-model differences as might occur in a realistic suite of models, such as the IPCC set. To construct a realistic experiment with toy models, a correspondence was established between parameter differences among the toy models on the one hand, and differences among models or parameters used in actual climate projection on the other. It was argued in [4] that differences in the forcing coefficient μ_0 in the QG models are analogous to differences in climate model sensitivities to increased greenhouse gas levels. The latter sensitivities are known to vary among IPCC models by about $\pm 1/3$ of the average value. Considering proportional variations in μ_0 in the range $0.2 < \mu_0 < 0.4$, instead of the extreme range $0 < \mu_0 < 3.0$ used above, it was found that a weighted average of their blocking frequencies could reproduce the "true" behavior. At least in regard to blocking frequency, the advantage of supermodeling is lost in this less extreme case.

If one pays more attention to the detailed modes of variability, a subtle advantage remains. It is known that there is a very weak anticorrelation between blocking activity in the Atlantic and in the Pacific [7]. That effect could not possibly occur in an output-average of models with Atlantic and Pacific forcing separately. It is thought that supermodeling will give improved predictions of other global multi-variable patterns of variability, where the relationships are stronger, as well.

IV. Supermodeling with Primitive Equation Models

A supermodel containing the main dynamical ingredients or real climate model was constructed from several versions of the intermediate complexity model SPEEDO [23]. The atmospheric component is the SPEEDY model that solves the primitive equations on a sphere using a spectral method. The spectral expansion is truncated at total wavenumber 30 which corresponds to a spatial resolution at the equator of about 500 km. It has 8 vertical levels and simple parameterizations for radiation, convection, clouds and precipitation The solar radiation follows the seasonal cycle but the diurnal cycle is not imposed. Instead daily mean solar radiation fluxes are prescribed. The total number of degrees of freedom is 38025: 31680 for the spectral coefficients of divergence, vorticity, temperature, specific humidity and log of surface pressure plus 6345 to describe the land temperature, land moisture and snow cover in the 2115 land points. The land component uses a simple bucket model to close the hydrological cycle over land and a heat budget equation that controls the land temperatures. The ocean component is the CLIO model [11]. The CLIO model is a primitive-equation, free-surface ocean general circulation model coupled to a thermodynamic-dynamic sea-ice model. The ocean component includes a relatively sophisticated parameterization of vertical mixing. A three-layer sea-ice model, which takes into account sensible and latent heat storage in the snow-ice system, simulates the changes of snow and ice thickness in response to surface and bottom heat fluxes. In the computation of ice-dynamics, sea ice is considered to behave as a viscous-plastic continuum. The horizontal resolution of CLIO is 3 degrees in latitude and longitude and there are 20 unevenly spaced vertical layers in the ocean. The CLIO model has a rotated grid over the North Atlantic ocean in order to circumvent the singularity at the pole. The total number of degrees of freedom is on the order of 200,000.

Three SPEEDY atmospheres, with different parameters chosen to reflect the typical range of behavior of different atmospheric models, were coupled to the same ocean and the same land (see Fig. 7), and also to one another, by adding inter-atmosphere coupling terms to the dynamical equations for each atmosphere. The modified equation for the temperature field for model i (i = 1 . . . 3), for instance, is:

$$\partial T_i/\partial t = (RT_i/c_p)(\sigma\dot{}_i/\sigma_i - \partial\sigma\dot{}_i/\partial\sigma_i - \nabla \cdot V_i) + \Sigma_{js}[C^{ij}_s(T_j - T_i)\,\delta(x - x_S)] \quad (9)$$

where all variables are evaluated at position x and $\{x_S\}$ is a set of discrete coupling points. In (9), R is the gas constant, c_p is the specific heat at constant pressure, σ is a vertical pressure coordinate scaled with surface pressure, $\sigma\dot{}$ its time-derivative, V is the horizontal wind velocity, and C^{ij} is a connection coefficient linking the temperature fields between models i and j at position x_S. Dynamical equations for the other independent variables, u (east-west velocity), v (north-south velocity), and q (humidity) are similarly modified to include coupling terms linking the different models.

In the present situation, regarding the PDE as a very high-order ODE, the general rule for adaptation of parameters (2), as applied to the connection coefficients C^{ij}, gives:

$$dC^{ij}/dt = a \int dx\,(T_j(x) - T_i(x))(T^t(x) - \tfrac{1}{3}\Sigma k\, T_k(x)) \quad (10)$$

where T^t is the true value of T, and *a* is an arbitrarily chosen learning rate. We assume spatially uniform connections C^{ij} that are independent of position s. Analogous rules are written to adapt the connections linking the other dynamical variables, with learning rates appropriate for their dynamics. The algorithm was tested by choosing one of the models to be a perfect replica of the "true" system; appropriate binary values for the connections did indeed result. All models are nudged to truth as the learning progresses; for the configuration studied, it was found that nudging to truth in the *u* field gave truth-model synchronization error rates that were useful in discriminating between good and bad models, so that the learning algorithm was effective.

Note that the last term in (9), connecting the models, tends to vanish as the models synchronize. This is desirable, so that each model satisfies its own physically motivated dynamical equation, without the influence of artificial coupling terms. Of, course, for each i, the parameters and hence the equations are different, so that the models cannot possibly synchronize completely. Typically, the differences in behavior are in small-scale processes that are not important for the large-scale behavior of interest.

The system was tested with the three arbitrarily chosen imperfect models of a "true" SPEEDO system, assuming ongoing nudging of the models to the "true" system, as if doing weather prediction with continuous data assimilation [6]. The "true" system also provided the land and ocean components for each of the imperfect models. Results are shown for the simple case of two identical models and a different third model in Fig. 8. It is seen that after 3 months, the truth-supermodel error, with adapted coefficients, is less than the error for each of the individual models, and less than the error for the supermodel with a choice of uniform connection coefficients that are not adapted.

Then the coefficients were frozen and atmospheric CO2 was doubled in the "true" system and in each of the models. Other parameters were also varied slightly. Results are shown in Fig. 9. It is seen that the supermodel gives reduced error after three months as compared to the weighted averages of the separate models, but the coefficients learned from the single-CO2 runs are less than optimal. That is, a simple choice of uniform coefficients gives slightly better results than the learned coefficients (in this artificially constructed case where the imperfect models were about equally spaced around the true models), but the model with learned coefficients was still effective. Thus the supermodel is not only useful for exploring state space, but also for exploring an enlarged model space defined by variations in ancillary parameters.

V. A Weakly Connected Supermodel Formed From Full Climate Models Connected Only At the Ocean-Atmosphere Interface

Investigations with full climate models have thus far reached a stage in which different atmosphere models are connected to a common ocean, as in the early work of Kirtman [15] but not directly connected to each other. Yet even without the direct connections, the supermodel has been shown to be superior to any weighted combination of outputs of the individual models [24].

A climate model was built based on COSMOS (ECHAM5/MPIOM, developed at the Max-PlanckInstitut fur Meteorologie, Germany [12], and involved two atmospheric general circulation models (AGCMs). The two models differed in their cumulus parameterization schemes, Nordeng [21] and Tiedtke [26], to represent typical model diversity because cumulus convection schemes normally have a strong impact on the climate state [14,16,18]. The ocean model continuously interacts with the Nordeng atmosphere and Tiedtke atmosphere. AGCMs are problematic in representing real air-sea fluxes to different degrees of accuracy. Some may be better in representing momentum flux (i.e. wind stress on the ocean) and some in energy (heat) flux [15]. Different weights were used for the energy, momentum, and mass (i.e. precipitation) fluxes felt by the common ocean, with the sum of the weights over the two models, for each type of flux, equal to unity. Each atmosphere feels only its own fluxes.

A machine learning technique, the Nelder-Mead method [20] was applied to optimize the weights for each of the fluxes. The Nelder-Mead method is also known as the simplex method, which is used to find a local minimum in multi-dimensional domain without having to compute gradients of a cost function. A performance index [22] computed over the Pacific region (160°E − 90°W, 10°S − 10°N), was used as a metric because there is partial synchronization over the tropical Pacific in this configuration; hence it is reasonable to expect that improvement can only be achieved over this area. The assessment was started from equal weights and followed the weights suggested by the simplex method. Each case was spun up

for ten years and run for another 30 years to get a reasonable climatology. Over 300 cases were tested along the path to optimal weights, for which the performance index (error) was reduced and the correlation between zonal wind stress anomaly of two AGCMs is increased. Note that the variability of AGCMs tends to cancel over non-synchronized areas, thus reducing the ocean variability as well.

The behavior predicted by the supermodel was dramatically improved as shown in Figure 10, in which both the SST and precipitation have better agreement with observations. The cold tongue is stopped around the International Date Line, which suggests that a west-Pacific warm pool was formed in the supermodel, unlike the situation in COSMOS(N), COSMOS(T), or their averaged output, COSMOS(E), in all of which the cold tongue crossed the International Date Line to the western Pacific and the variability of SST is much larger (not shown). The supermodel largely mitigates the double ITCZ error found in both COSMOS models and in most climate models.

The reduction of the SST bias in the supermodel implies that the whole dynamic is more realistic, suggesting that a much more realistic low level wind system exists in the supermodel, leading to a better latitudinal position of the Inter-tropical Convergence Zone (ITCZ). But it is still too wet in the South Pacific convergence zone.

The key to improved supermodel performance in this case appears to be in better representation of the air-sea feedbacks. In Figure 11, we show the Bjerknes feedback and the thermodynamic feedback for the supermodel (SUMO), the individual models, and observations. The Bjerknes feedback in the supermodel is almost perfect and the thermodynamic feedback is much improved.

It can be shown that the supermodel is superior to any weighted combination of the two model outputs. In Fig. 12, we present a Taylor diagram that shows the correlation between model and observations, as well as the normalized standard deviation of the model field, for the various models. It is seen that the supermodel has almost the same standard deviation of SST as in the observed data, unlike any of the models, and the correlation coefficient is higher.

An objection to supermodeling in the meteorological community is that ensembles of model runs (where the models are the same or different) are usually used to estimate spread as an indication of error. One loses this information with supermodeling if the models synchronize nearly completely. However, the ensemble of models in the usual practice can be replaced by an ensemble of weights. One can examine the learning history, or simply look at the performance metric for a random sample of weights, to infer a plateau in weight space along which the performance is close to optimal. Then weights on that plateau can be used to define an ensemble of supermodels. Results of this procedure, shown in Fig. 13 give a plausible ensemble of SST fields. The models effectively “agree to disagree”.

VI. Conclusions

The supermodel scheme for the fusion of imperfect computational models is not limited to climate models. Supermodeling only requires that the constituent models come equipped with a procedure to assimilate new measurements from an objective process in real time and, hence, from one another. The scheme could thus also be applied to financial, physiological or ecological models. It has been speculated that the mind could also be conceived fundamentally as a supermodel, perceiving/synchronizing with the objective world, but also with a capacity for interaction among semi-autonomous components and resulting self-perception commonly experienced as consciousness [5].

Specific studies demonstrated that a wide range of coupling schemes and connection strengths will lead to inter-model synchronization and hence consensus. Conversely, in situations with a high degree of nonlinearity in the dynamics, synchronization is essential - the inter-model connections are needed to give results surpassing those of output averaging. Indeed the fact that a supermodel, in which the constituent models are themselves synchronized, will in turn readily synchronize with an objective process, is an instance of a more general hypothesis about the relationship between internal and external synchronization [2,5]. The choice of semi-autonomous models to be combined is not essential, as long as the "gene pool" of models is diverse.

It is interesting that in both the quasigeostrophic supermodel described in Section III and the COSMOS supermodel described in Section V, the constituent models err on the same side of reality, with an absence of blocking in the former case and an anomalous cold tongue in the latter one. Where there is such non-monotonic behavior, some type of weighted supermodel, and probably a connected supermodel, are guaranteed to outperform an output average. The commonality of such non-monotonic behavior is not yet clear. But perhaps a principle akin to that of self-organized criticality [1] is at work – when all scales are represented dynamically, the model naturally gravitates to some kind of critical state, a behavior that must be manually inserted in parameterized models or learned. The supermodel reduces the dimensionality of the learning problem by exploiting human experience to isolate the dimensions along which arbitrary choices tend to be made.

Synchronization, to whatever degree it is present, implies that the supermodel can be viewed more as a single model than as an ensemble of models. Thus detailed features will survive that would be washed out in an output average. However, in many applications one is only interested in statistical properties of these features, many of which are adequately represented by an average of the statistics of the separate systems. The degree of model nonlinearity in realistic situations will determine the advantage of supermodeling for capturing the structures of interest, or higher-order statistical properties thereof.

References

1. Bak, P., Tang, C., and Wiesenfeld, K.: Self-organized criticality: an explanation of 1/f noise, *Phys. Rev. Lett.* 59, 381-384 (1987)

2. Duane, G.S.: Synchronization of extended systems from internal coherence. *Phys. Rev. E* 80, 015202 (2009)

3. Duane, G.S.: Data Assimilation As Artificial Perception and Supermodeling As Artificial Consciousness. In: Consensus and Synchronization in Complex Networks, Kocarev, Ljupco (Ed.), Springer (2013)

4. Duane, G.S.: Report on activities and findings under DOE grant "Collaborative research: An Interactive Multi-Model for Consensus on Climate Change" #DE-SC0005238 (2015)

5. Duane, G.S.: Synchronicity from synchronized chaos, *Entropy* 17, 1701-1733 (2015)

6. Duane, G.S. and Selten, F.: Supermodeling by synchronization of alternative SPEEDO models, Paper presented at *EGU General Assembly*, No. 15945, Vienna, Austria, April 2016

7. Duane, G.S. and Tribbia, J.J.: Weak Atlantic-Pacific teleconnections as synchronized chaos, *J. Atmos. Sci.* 61, 2149-2168 (2004)

8. Duane, G. S, Tribbia, J., and Kirtman, B.: Consensus on long-range prediction by adaptive synchronization of models. Paper presented at *EGU General Assembly*, No. 13324, Vienna, Austria, April 2009

9. Duane, G.S., Tribbia, J.J., and Weiss, J.B.: Synchronicity in predictive modeling: A new view of data assimilation, *Nonlin. Processes Geophys.* 13, 601-612 (2006)

10. Duane, G.S., Yu, D.-C., Kocarev, L.: Identical synchronization, with translation invariance, implies parameter estimation, *Phys. Lett. A* 371, 416–420 (2007)

11. Goosse H. and Fichefet, T.: Importance of ice-ocean interactions for the global ocean circulation: a model study, *J. Geophys. Res.* 104, 23337-23355 (1999)

12. Jungclaus, J. H., Keenlyside, N., Botzet, M., Haak, H., Luo, J.-J., Latif, M., Marotzke, J., Mikolalewicz, U., and Roeckner, E.: Ocean Circulation and Tropical Variability in the Coupled Model ECHAM5/MPI-OM, *J. Climate* 19, 3952–3972 (2006)

13. Kalnay, E.: Atmospheric Modeling, Data Assimilation, and Predictability, Cambridge Univ. Press, Cambridge (2003)

14. Kim, D. Yang, Y.-S., Kim, D.-H., Kim, Y.-H., Watanabe, M., Jin, F.-F., and Kug, J.-S.: El Nino-Southern Oscillation Sensitivity To Cumulus Entrainment In A Coupled General Circulation Model, *J. Geophys. Res.* 116, D22112 (2011)

15. Kirtman, B. P., Min, D., Schopf, P. S., and Schneider, E. K.: A New Approach for Coupled GCM Sensitivity Studies, *COLA Technical Report No.* 154 (2003)

16. Klocke, D., Pincus, R., and Quaas, J.: On Constraining Estimates of Climate Sensitivity with Present-Day Observations through Model Weighting, *J. Climate* 24, 6092– 6099 (2011)

17. Lorenz, E.N. : Deterministic non-periodic flow, *J. Atmos. Sci.* 20, 130–141 (1963)

18. Mauritsen, T. *et al.*: Tuning the Climate of A Global Model, *J. Adv. Model. Earth Syst.* 4, M00A01 (2012)

19. Mirchev, M., Duane, G.S., Tang, W.S., and Kocarev, L.: Improved modeling by coupling imperfect models, *Commun. Nonlinear Sci. Numer. Simul.* 17, 2471–2751 (2012)

20. Nelder, J. A. and Mead, R: A Simplex Method for Function Minimization, *The Computer Journal* 7, 308–313 (1965)

21. Nordeng, T.-E.: Extended Versions of the Convective Parametrization Scheme at ECMWF and Their Impact On the Mean and Transient Activity of the Model in the Tropics, *Technical Memorandum* No. 206, European Centre for Medium Range Weather Forecasts (1994)

22. Reichler, T. and Kim, J.: How Well Do Coupled Models Simulate Today's Climate?, *Bull. Amer. Meteor. Soc.* 89, 303–311 (2008)

23. Severijns, C. and Hazeleger, W.: The efficient global primitive equation climate model Speedo., *Geoscientific Model Development Discussions* 2, 1115–1155 (2009)

24. Shen, M.-L., Keenlyside, N., Selten, F., Wiegerinck, W., and Duane, G.S.: Dynamically combining climate models to "supermodel" the Tropical Pacific, *Geophys. Res. Lett.* 43, 359-366 (2016)

25. Tebaldi, C. and Knutti, R.: The use of the multi-model ensemble in probabilistic climate projection, *Philos. Trans. R. Soc. A* 365, 2053–2075 (2007)

26. Tiedtke, M.: A Comprehensive Mass Flux Scheme for Cumulus Parameterization in Large-Scale Models. Monthly Weather Rev. 117, 1779–1800 (1989)

27. van den Berge, L.A., Selten, F.M., Wiegerinck, W. and Duane, G. S.: A multi-model ensemble method that combines imperfect models through learning, *Earth Systems Dynamics* 2, 161-177 (2011)

28. Vautard, R. and Legras, B.: On the source of mid-latitude low-frequency variability. Part II: Nonlinear equilibration of weather regimes, *J. Atmos. Sci.* 45, 2845-2867 (1988)

29. Vautard, R., Legras, B., and Déqué, M.: On the source of mid-latitude lowfrequency variability. Part I: A statistical approach to persistence, *J. Atmos. Sci.* 45, 2811–2843 (1988)

30. Wiegerinck, W., Burgers, W., and Selten, F.: On the Limit of Large Couplings and Weighted Averaged Dynamics. In: Consensus and Synchronization in Complex Networks, Kocarev, Ljupco (Ed.), Springer (2013)

31. Yang, S.-C., Baker, D., Cordes, K., Huff, M., Nagpal, G., Okereke, E., Villafan˜e, J., and Duane, G.S. : Data assimilation as synchronization of truth and model: Experiments with the three- variable Lorenz system, *J. Atmos. Sci.* 63, 2340-2354 (2004)

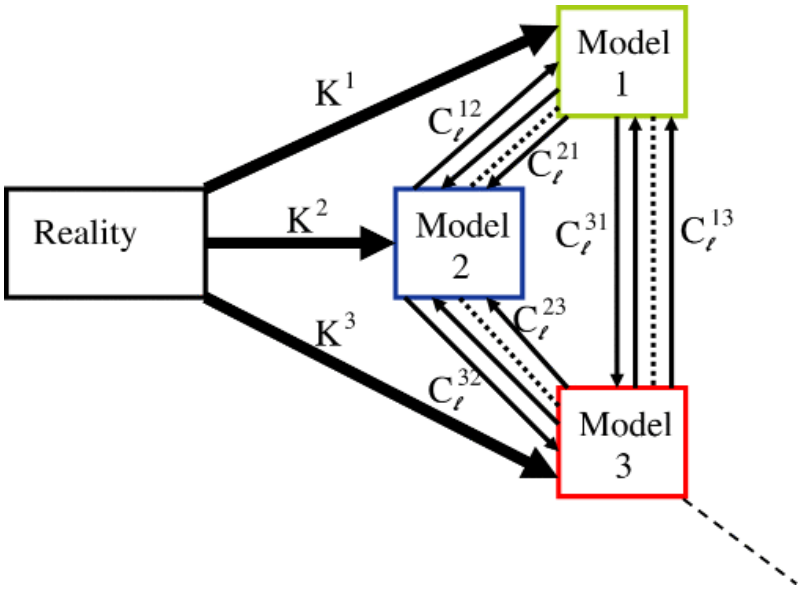

Figure 1. In a supermodel, models are linked to each other, generally in both directions and to "reality" in one direction. Separate links between models, with distinct values of the connetion coefficients C^{ij}_l, are introduced for different variables and for each direction of possible influence.

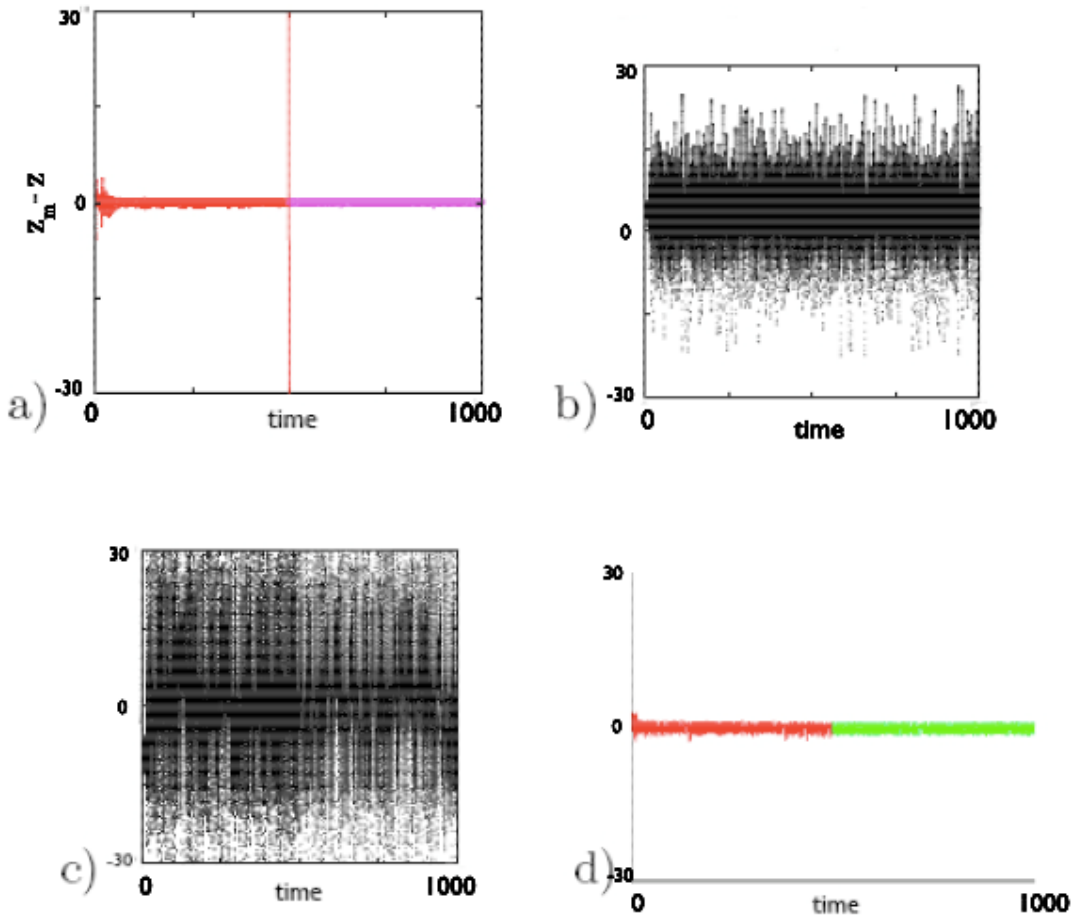

Figure 2. Difference $z_m - z$ between "model" and "real" z *vs*. time for a Lorenz system with $\rho = 28$, $\beta = 8/3$, $\sigma = 10.0$ and an interconnected suite of models with $\rho_{1,2,3} = \rho$, $\beta_1 = \beta$, $\sigma_1 = 15.0$, $\mu_1 = 30.0$, $\beta_2 = 1.0$, $\sigma_2 = \sigma$, $\mu_2 = -30.0$, $\beta_3 = 4.0$, $\sigma_3 = 5.0$, $\mu_3 = 0$. The synchronization error is shown for (a) the average of the coupled suite $z_m = (z_1+z_2+z_3)/3$ with couplings C^A_{ij} adapted according to (3) for $0 < t < 500$ and held constant for $500 < t < 1{,}000$; (b) the same average z_m, but with all $C^A_{ij} = 0$; (c) $z = z_1$, the output of the model with the best z equation, with $C^A_{ij}=0$; (d) as in (a), but with $\beta_1 = 7/3$, $\sigma_2 = 13.0$, and $\mu_3 = 8.0$, so that no equation in any model is "correct".

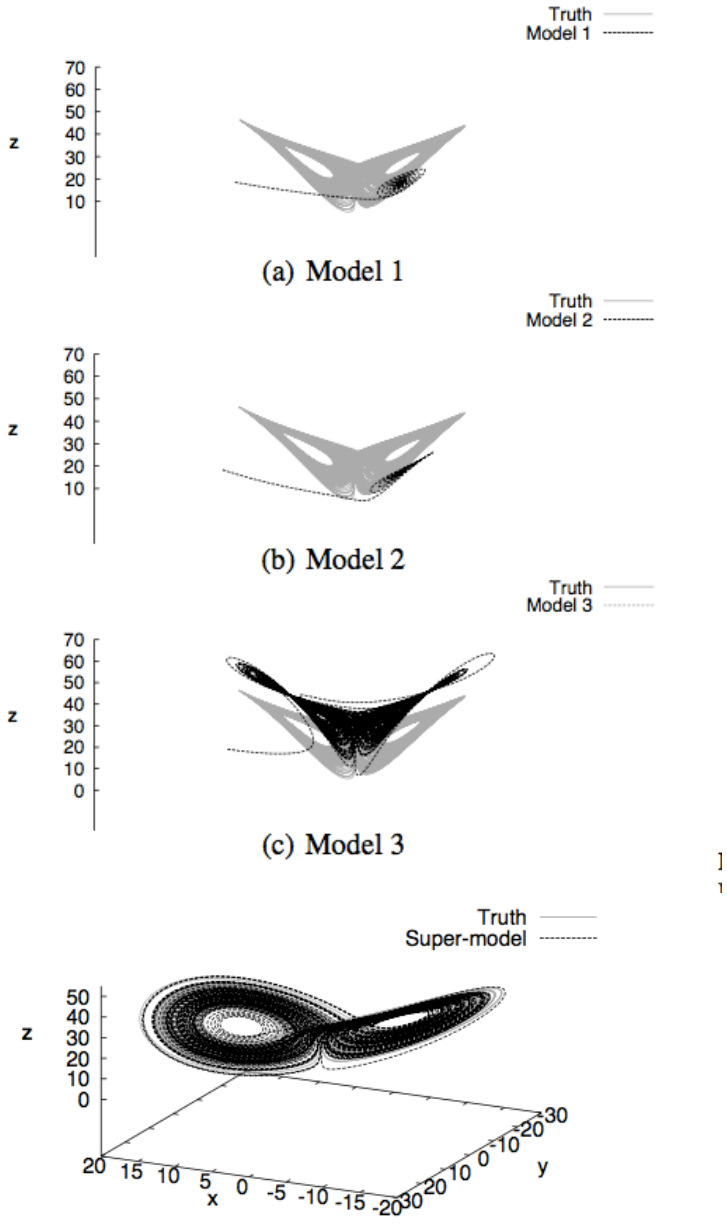

Figure 3. (a,b,c) Trajectories for the three unconnected imperfect models (black) and for the "true" Lorenz system (grey). The trajectories include an initial transient as well as the attractor. (d) Trajectories for the supermodel (black) trained by minimizing the cost function (4), and for the true Lorenz system (grey).

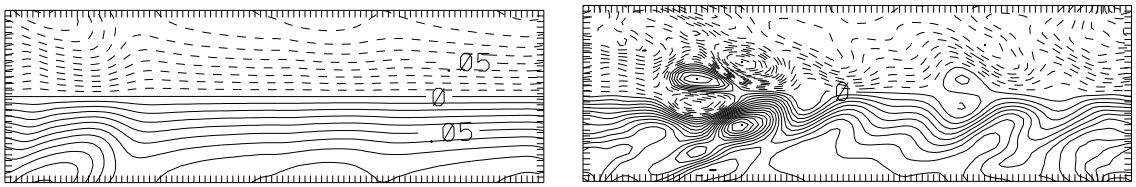

a) CONTOUR FROM −.11 TO .11 BY .01 b) CONTOUR FROM −.075 TO .075 BY .005

Figure 4: Streamfunction (in dimensional units of $1.48\times10^{9}\mathrm{m}^{2}\mathrm{s}^{-1}$) describing a typical zonal flow state (a), and a typical blocked flow state (b) in the two-layer quasigeostrophic channel model. Parameter values are as in (Duane and Tribbia , 2004). An average streamfunction for the two vertical layers i = 1,2 is shown.

a) 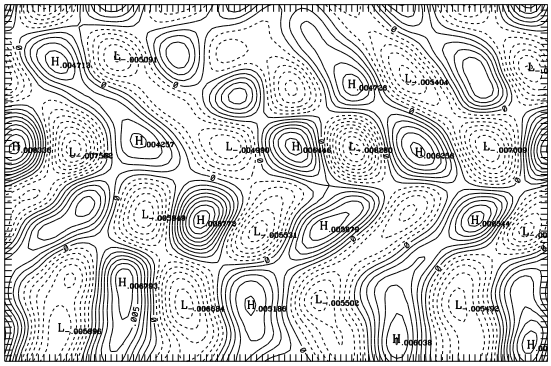

b) 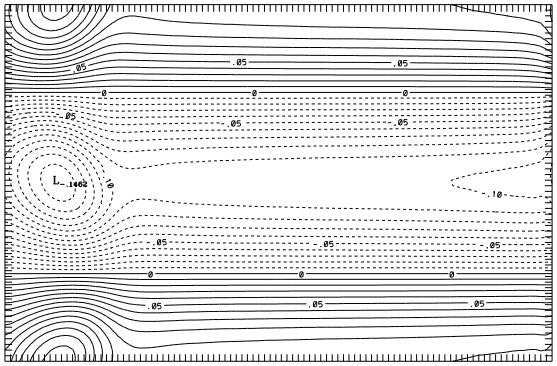

Figure 5: Typical flows in the QG channel model with very small forcing coefficient ($\mu_0 = 0$) (a), and very large forcing coefficient ($\mu_0 = 3.0$) (b). (The spatial domain in each panel includes two channels with flows in opposite directions).

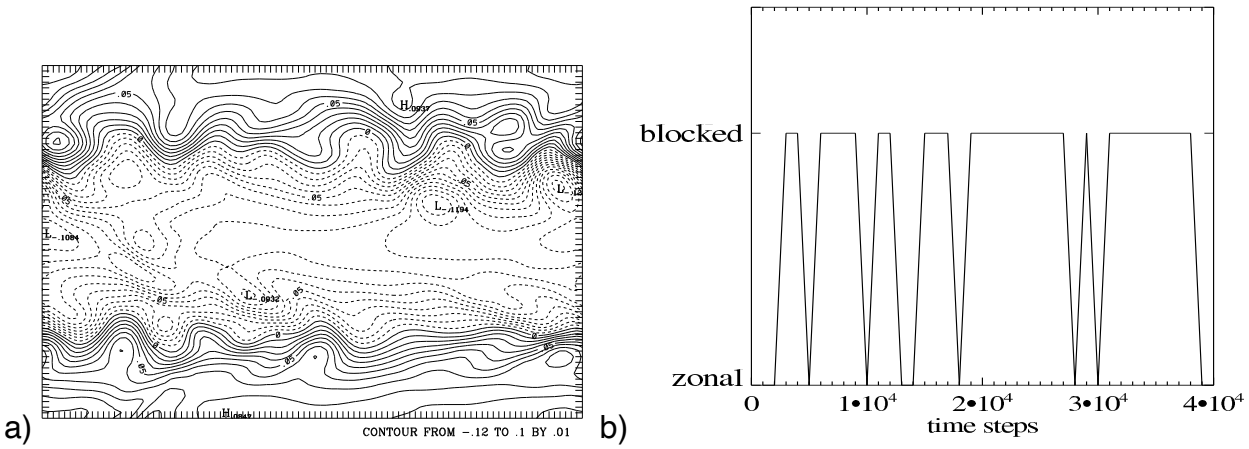

Figure 6: Typical flow in the QG channel model with a "realistic" forcing coefficient (μ_0 = 0.3) (a), and the history of vacillation of the flow in the bottom half of the domain between zonal and blocked regimes, sampled at low temporal resolution over the course of a simulation (b), using the blocking diagnostic defined in (Duane and Tribbia , 2004). The typical flow is also the exact solution to an appropriately weighted supermodel.

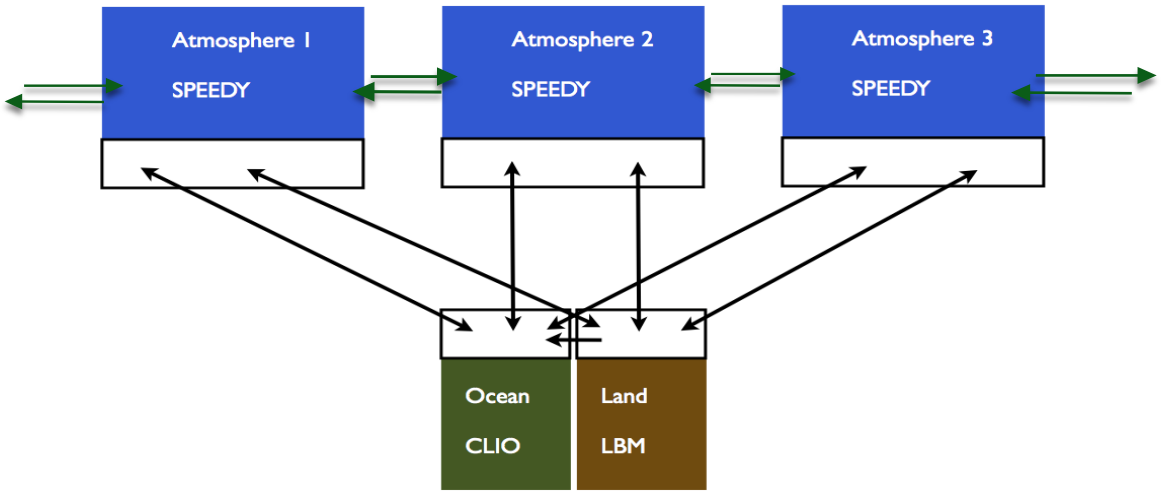

Figure 7. Schematic representation of SPEEDO supermodel. The Ocean and Land models are the "true" Ocean and Land, resp.

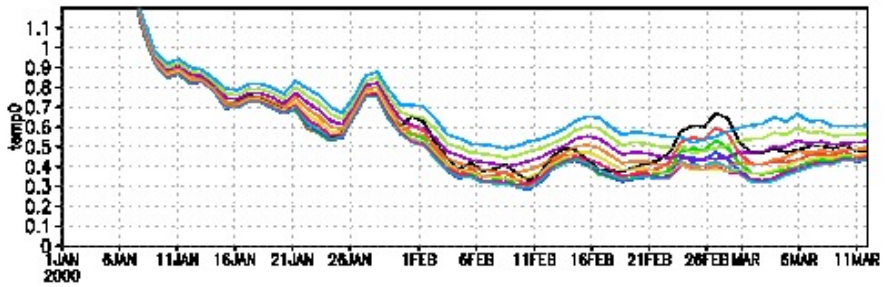

a)

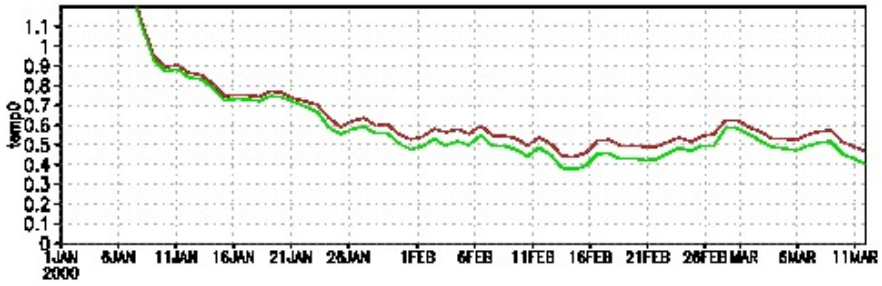

b)

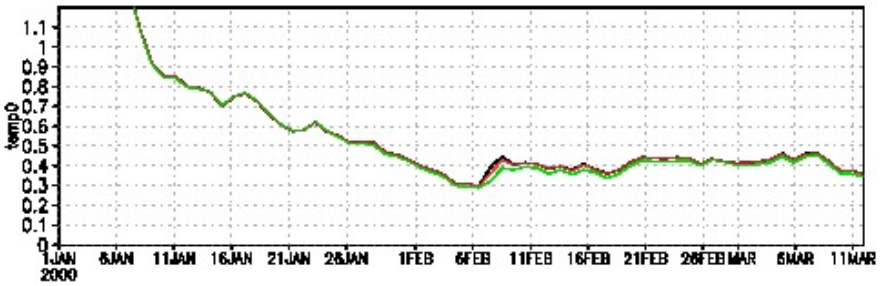

c)

Figure 8: Truth-model synchronization error in surface temperature (in $^{\circ}$C) for a) three SPEEDO models with parameters perturbed away from their values in a "true" SPEEDO model to which the imperfect models are nudged via the u variable (with two of the models identically perturbed) and various weighted combinations of their outputs; b) a supermodel formed by connecting the three SPEEDO models through their dynamical equations according to Eq.(5) (for temperature) and analogous equations for u, v, and q, with constant and uniform connection coefficients C^{ij}; and (c) the same supermodel but with connections adapted according to (6) with analogous equations for the u, v, and q connections.

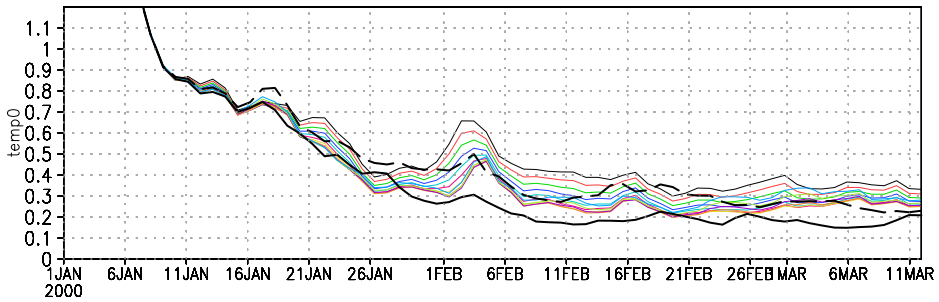

a)

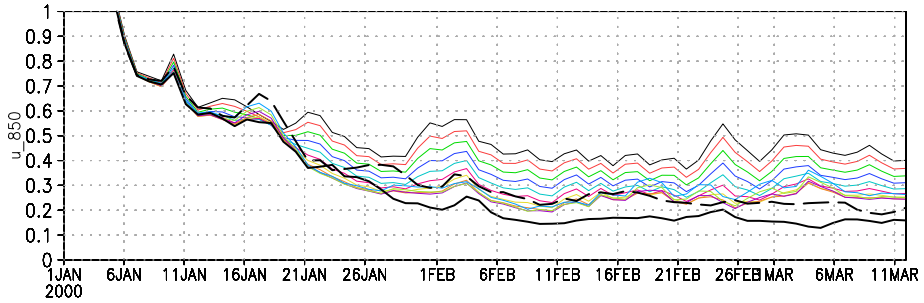

b)

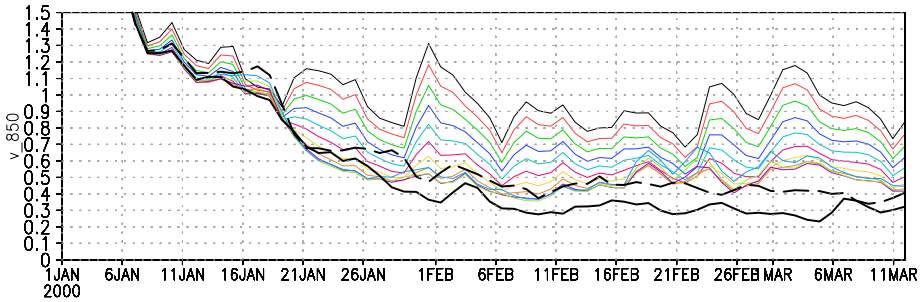

c)

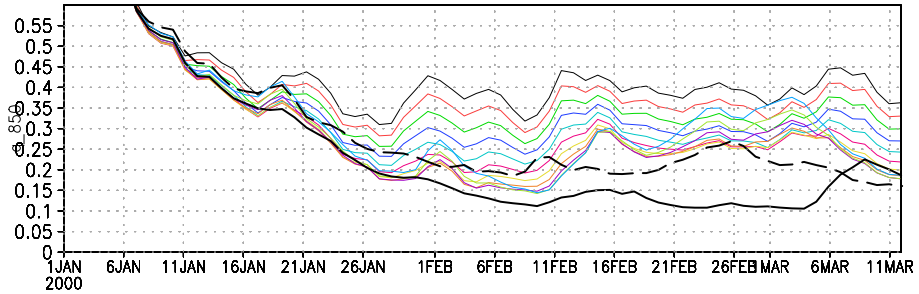

d)

Figure 9: Truth-model synchronization error in surface temperature (in $^{\circ}$C) a) for three SPEEDO models as in Fig. 7, but with doubled CO2 in both truth and models, for various weighted combinations of model outputs (colored lines), a supermodel with uniform connections (thick black line), and a supermodel using the connection strengths from the present-CO2 run (Fig. 7c) at final time (dashed). Correspondingly for error in zonal wind u at 850 mb (b), error in meridional wind v at 850 mb (c), and error in humidity q (d)

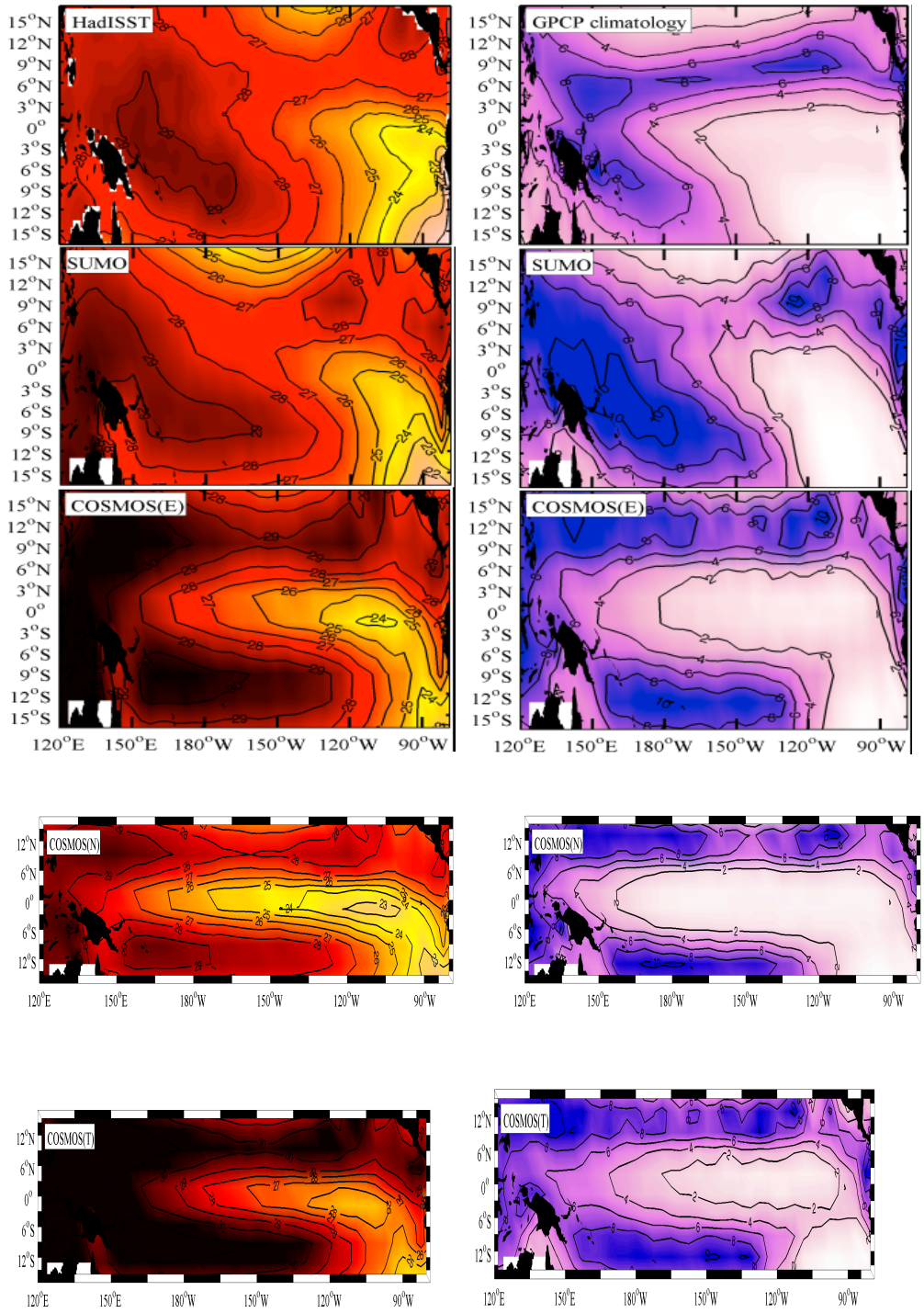

Figure 10: The climatology sea-surface temperature (SST) (left panel, scale in °C) and precipitation (right panel, scale in mm/day) in the Tropical Pacific from observations, the trained supermodel (SUMO), the untrained, equal-weighted supermodel (COSMOS(E)) and the two constituent models, COSMOS(N) and COSMOS(T). Observed SST is from HadISST (1948-1979, the period used as a training set) while observed precipitation is from GPCP (1979-2012, due to the available data). Because the SST state over the equator is improved in the supermodel (SUMO), there is one ITCZ in SUMO.

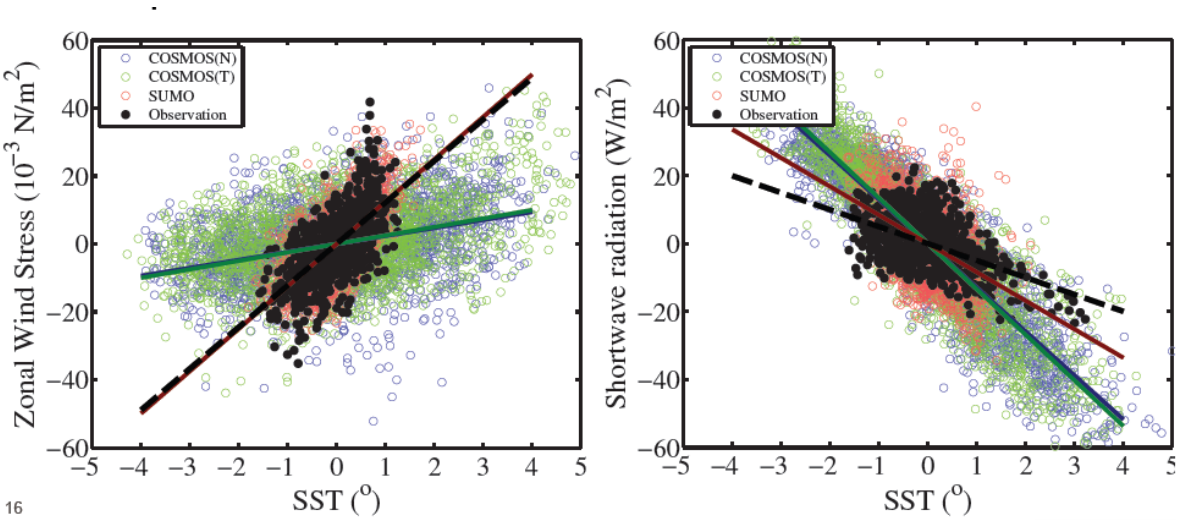

Figure 11: (a) The Bjerknes feedback (left panel), describing the relationship between the east Pacific SST anomaly (over 5°S-5°N, 150°W-90°W, Niño 3 region) and the remote wind stress over the west Pacific (5°S-5°N, 160°E-150°W, Niño 4 region); (b) the thermodynamic damping (right panel) over the Niño 3 area. Coefficients of regression and correlation are included in the legend.

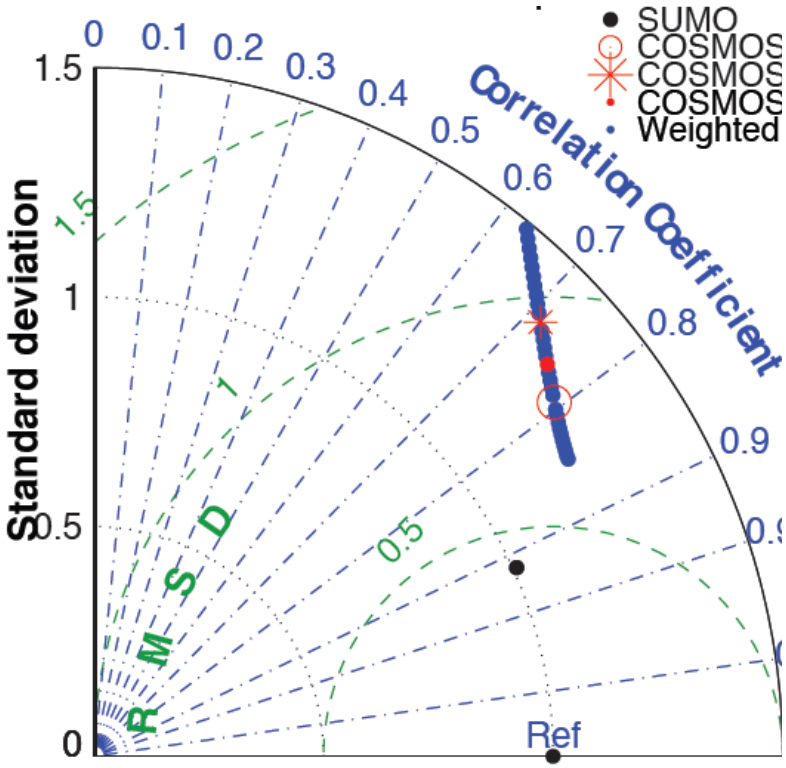

Figure 12: Taylor diagram showing the correlation between observed and modeled SST over the Tropical Pacific, as well as the normalized standard deviation, for COSMOS(N), COSMOS(T), their equal-weighted combination COSMOS(E), all other weighted combinations (thick line), and the supermodel (SUMO). SUMO is clearly closer to observations (Ref) than any weighted average.

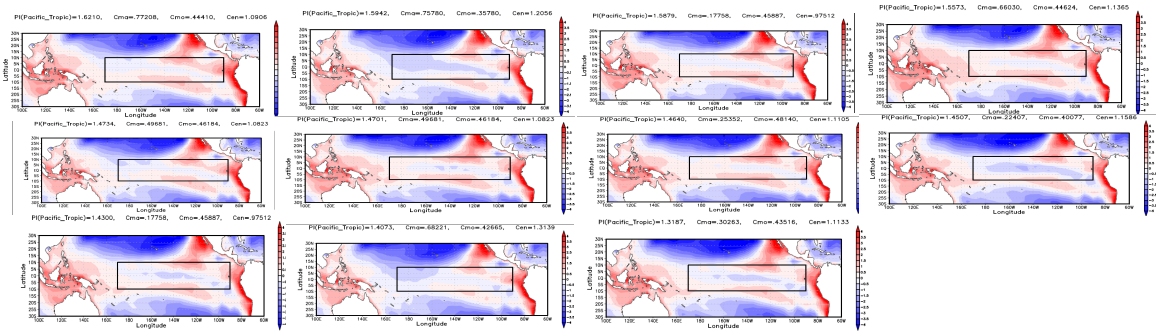

Figure 13: SST fields for an ensemble of supermodels defined by examining the learning history to select combinations of weights that give near optimal performance, each of which defines a different supermodel, giving a plausible spread in results.